

Contents lists available at [ScienceDirect](https://www.sciencedirect.com)

Optik

journal homepage: [www.elsevier.com/locate/ijleo](http://www.elsevier.com/locate/ijleo)

Original research article

## Measurement of moisture content in lubricating oils of high-speed rail gearbox by Vis-NIR spectroscopy

Chenyang Liu<sup>a,b</sup>, Xingjia Tang<sup>c</sup>, Tao Yu<sup>c</sup>, Taisheng Wang<sup>a</sup>, Zhenwu Lu<sup>a</sup>,  
Weixing Yu<sup>c,\*</sup>

<sup>a</sup> R&D Center of Precision Instruments and Equipment, Changchun Institute of Optics, Fine Mechanics & Physics, Chinese Academy of Sciences, No. 3888, Dongnanhu Road, Changchun, Jilin, China

<sup>b</sup> University of Chinese Academy of Sciences, Beijing 100049, China

<sup>c</sup> Key Laboratory of Spectral Imaging Technology, Xi'an Institute of Optics and Precision Mechanics, Chinese Academy of Sciences, No. 17, Xinxu Road, Xian 710119, China



### ARTICLE INFO

#### Keywords:

Vis-NIR spectroscopy  
Lubricating oils  
Moisture content  
The reflection probe  
Successive projections algorithm  
Partial least square regression  
Back propagation neural network

### ABSTRACT

The moisture content in lubricating oil is one of the most important factors to reflect the health and effectiveness of it, thus to monitor the moisture content in lubricating oil in real time is crucial for high speed rail. In this paper, we developed a compact moisture-content monitoring system based on the visible-near-infrared (Vis-NIR) spectroscopy technology, which was shown to be able to determine the moisture content in lubricating oil in a fast, simple and accurate way. In this system, a reflection mode optical probe was developed for sending and receiving optical signals through the viewport of gear box. By employing the reflection optical probe, one can measure the spectrum of the lubricating oil in a fast way by simply putting the probe on viewport of gear box, and therefore has the potential to realize the real-time monitoring of the status of the lubricating oil. In order to verify the feasibility of the system, both reflection and transmission spectral of lubricating oil were taken. Partial least square regression (PLS) and back propagation neural network (BPNN) algorithms were used to establish the processing model. Modelling results show a good agreement in between two different probing modes. As a result, the effectiveness and reliability of the system have been proved, which provides a simple yet accurate method for real time monitoring the healthy status of the lubricating oil for the safe operation of the high-speed rail.

### 1. Introduction

High speed rail trains now play an important role in Chinese modern life and have become a great factor to promote the economic growth in China. Safety and reliability are crucial for high speed rail train service. The gearbox as a key transmission component of a high-speed train traction system is used for transmitting the motor torque to the axle. Its reliability is directly related to the operational safety of the high-speed train [1,2]. Lubricating oil as a mechanical 'blood', plays an important role in the smooth and long-life operation of the gearbox [3,4]. However, lubricating oil suffers from contaminating from both internal frictions caused by bearings in gearbox and also from external environment due to the change in temperature and humidity. Especially in China, the season change

\* Corresponding author.

E-mail address: [yuwx@opt.ac.cn](mailto:yuwx@opt.ac.cn) (W. Yu).

<https://doi.org/10.1016/j.ijleo.2020.165694>

Received 7 May 2019; Received in revised form 24 June 2020; Accepted 23 September 2020

Available online 28 September 2020

0030-4026/© 2020 Elsevier GmbH. All rights reserved.

due to the long span of the railway results in a great change in temperature and humidity of ambient air, which makes the pollution on lubricating oil unavoidable. Therefore, it is very necessary to monitor the condition of the lubricating oil to guarantee the safety of the high-speed rail. In recent years, more and more researchers pay attention to the detection of contaminants in lubricating oil [5–14]. Water is one of the most destructive contaminants in lubricants. It can act directly on metal bearing surfaces and also can decrease lubricant effectiveness [9]. As a result, the ultimate manifestations of water contamination in lubricants are corrosion, excessive wear and premature failure of lubricated metal bearing surfaces. Therefore, it is vital to monitor and quantify water contamination in the lubricating oil in order to ensure the safe service lifetime of the lubricants.

So far, a few of methods have been developed to test the moisture content in lubricating oil. The coulometric Karl Fischer titration is the most widely used method for determination water in petroleum products [15]. Nevertheless, it's not a non-invasive method and also quite time consuming. Fourier Transform Infrared (FTIR) Spectroscopy is a widely used method for moisture content measurement. However, FTIR spectrometer is quite complex and expensive, and thus only suitable for laboratory use [16,17]. Optical fiber sensor based on evanescent-field absorption combined with dielectrophoresis was also proposed and demonstrated to be an alternative method to determine the water content in lubricants [18]. But the implementation of this sensor needs to contact the oil with fiber and thus again is an invasive method like the Karl Fischer titration method. Raadnui et al. proposed a grid capacitance sensor method to determine the corresponding contaminants in lubricants by measuring the overall quality variations [19]. Although, the relative variation of the dielectric constant of lubricant caused by contaminants such as water, fuel dilution, wear debris, etc can be determined by this method, it is impossible to differentiate what kind of the specific contaminants are. As can be seen, aforementioned methods have the common limitations. Firstly, these methods either employs large equipment or needs to be implemented by well-trained operators and thus is more suitable for laboratory testing. Secondly, these methods need samples to be taken from gearbox for testing, which obviously makes frequently testing not possible due to the lubricating oil must be kept at some safe level. Therefore, above methods are not suitable for fast testing and thus not suitable for on-line monitoring so that a more portable and flexible method should be developed to meet this purpose.

Spectroscopy technology has been developing rapidly since Bouguer-Lambert-Beer developed a mathematical-based law for quantitative evaluation of spectral absorption measurement [20]. The spectral analysis method has been applied in the performance detection of lubricating oil, element content analysis in soil, food adulteration analysis, thermal decomposition of coal, fruit maturity and other aspects [3,13,21–25]. M Blanco, et al. demonstrated the measurement of water in lubricating oils for marine engines by near-infrared and mid-infrared spectroscopy method [8]. F. S. G Lima, et al. proposed to combine NIR spectroscopy with chemometrics technique to estimate on-line the carcinogenic potential of lubricant base oil, which was shown to be reliable, fast and inexpensive [26]. Zamora et al. developed a methodology based on NIR spectroscopy for the characterization and analysis of lubricant formulations [27]. Their method allows one to identify the components such as antioxidants and additives with similar spectra in lubricants.

In this work, we demonstrated the application of Visible-Near-Infrared spectroscopy method for determining the moisture content in lubricating oil for gearbox of high-speed rail train. Our project has two phases. The aim for the first phase is to develop a portable spectrometer for testing of moisture content in lubricating oil through viewport in gearbox. In the second phase, we aim to install the spectrometer onto the gearbox directly to realize real-time monitoring. This work is mainly to report our preliminary results about the portable apparatus and the data processing. Our preliminary results are promising, which shows clearly that the Visible-Near-Infrared spectroscopy method has the potential to be an ideal alternative method for real-time monitoring of the contaminating status of lubricating oil and thus to ensure the reliability of the gearbox for a safe high-speed rail operation.

## 2. Experimental section

### 2.1. Sample preparation

The fresh lubricating oils of gearbox for high-speed rail were provided by CRRC Qishuyan Co., LTD. Distilled water was added into the oil to act as the moisture contaminate. The dilution technique was used to prepare contaminated lubricating oil samples with

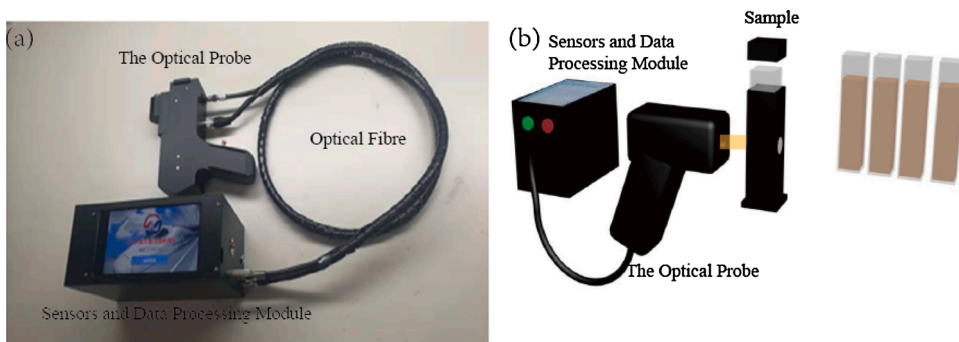


**Fig. 1.** The developed portable spectral measurement system (a) and the schematic diagram of the working principle for the moisture content measurement (b).

different moisture content from 100 ppm to 1500 ppm with an increase step of 100 ppm. Each sample was divided into 10 parts. As a result, a total of 150 samples were prepared. Before testing, the samples were shaken by hand for 10 min, followed by oscillated on the vortex mixer and in the ultrasonic for 10 min respectively. Once the samples were ready, they were tested by Vis-NIR spectroscopic method and Karl-Fisher method, respectively.

2.2. Vis-NIR spectroscopy method and instrument

A portable spectral detection system for real-time on-line analysis of gearbox lubricating oil is introduced. As shown in Fig. 1(a), the monitoring system consists of a light source, a visible and near-infrared spectrum module, a short-wave infrared spectrum module, the data analysis circuit, a display screen, a power supply and a data interface. The two spectrum modules share the same light source and the optical signals are transmitted by optical fibers. Fig. 1(b) shows the work principle of the portable spectral measurement system. Where, an optical fiber probe is used to collect the absorption spectrum of the sample. This kind of absorption spectrum is closely related to the content of the material in samples. Through appropriate regression algorithm, the content of the material can be inverted from the absorption spectrum. The data analysis circuit is responsible for the operation of regression algorithm. Then the inversion result is displayed on the display screen and can be exported through an USB interface. Vis-NIR spectra were measured in the transmittance mode and the reflectance mode separately on a spectrometer spliced from two INSION waveguide spectrometers. The wavelength range of visible short-wave spectrum module is 350nm~1100 nm, the optical resolution (FWHM) is 10 nm, the wavelength repeatability is 0.1 nm. And the wavelength range of the short-wave near-infrared spectral module is 900nm~1700 nm, the optical resolution (FWHM) is 16 nm, and the wavelength repeatability is 0.1 nm. The wavelength of 1100 nm is selected as the splicing point. The self-designed reflection probe in Fig. 1(b) will be described in detail later. Square quartz cuvettes with a 10 mm inner diameter were used to hold the sample oil. The tungsten halogen lamp was used as the light source. Then transmission method and reflection method are used to collect spectral data respectively. All samples were tested at room temperature (24 ± 1°C). The spectral analytical software was Matlab7.6.

The principle for measuring the oil contaminates is based on the Beer-Lambert law. The basic idea of Beer-Lambert law is that when a beam of parallel monochromatic light passes through a homogeneous medium, the portion of the incident light absorbed by the medium is proportional to the concentration of the absorbing medium and the length of the light path. The light absorbance can be calculated by,

$$A = -\log_{10}\left(\frac{I_t}{I_0}\right) = \epsilon \cdot c \cdot l \tag{1}$$

Where,  $A$  is the light absorbance with a dimensionless unit,  $I_t$  and  $I_0$  denote the transmitted light intensity and the incident light intensity respectively,  $\epsilon$  is the absorbance coefficient of the absorbing medium which has a unit related to the unit of  $c$ ,  $c$  is the concentration of the absorbing medium and  $l$  is the path length of the light passes through.

In reality, the relation between absorbance and concentration is usually non-linear, which can be attributed to two reasons. One is caused by the imperfect equipment, i.e. the light beam is not imperfectly collimated. The other reason lies in the medium, i.e. the medium is non-uniform and there could be chemical reactions during the measurement. In order to solve these two unavoidable problems, the chemometric method can be adopted to eliminate the influence of nonlinearity to some extent.

To meet the different measurement requirements and adapted to different working conditions, two optical probing system were developed by us, i.e. reflection and transmission measuring system. Fig. 2 shows the light path diagram for both systems. As can be

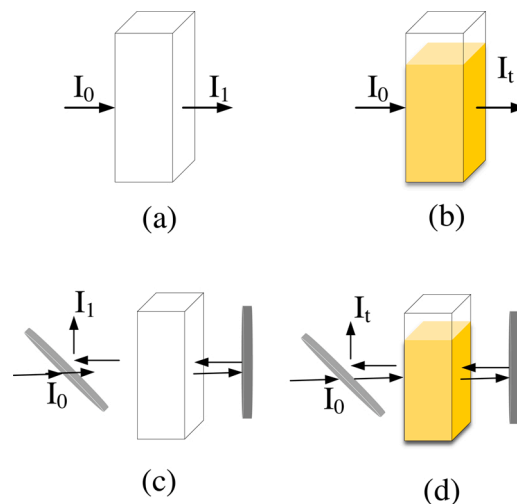


Fig. 2. The light path diagram for both transmission (a-b) and reflection (c-d) probe systems.

seen, the reflection probe system is like that of the transmission probe system except the light path is doubled. In practical cases, the reflection probe is more flexible than the transmission probe, as it only needs to align the probe perpendicularly to the surface of the liquid to do the measurement. Therefore, the reflection probe is more suitable to conduct on the viewport of the gearbox for lubricating oil test. In this work, two kinds of reflection probes were developed and they are shown in Fig. 3(a) and 3(b). In both reflection probes, the light is collimated first and then passes through a 50:50 beam splitter before propagating into the oil via viewport of the gearbox. The reflected light is then deflected by the beam splitter for an angle of 90° and received by the receiving fiber attached to the spectrometer. The only difference between two probes lie in the different collimators used. One uses a reflective collimating mirror and the other uses an optical fiber collimator. The effect of the collimator is key to the design which makes sure that the incident light incidents perpendicularly onto the viewport of the gearbox. At the same time the reflected light can also be gathered and focused onto the input end of the receiving fiber. As can be seen from Fig. 3, the red arrows represent the output light and the yellow arrows represent the input light which brings the spectrum information of the oil with contaminates. The reflection collimator is an off-axis parabolic mirror coated with silver film on its surface. The corresponding technique parameters of the reflection collimator are: the numerical aperture is 0.167, the reflective focal length is 33 mm, the beam diameter is 8.5 mm, and the average reflectivity is no less than 97.5 % at the whole working waveband ranging from 450–2000 nm. While for the optical fiber collimator, the corresponding parameters are: the numerical aperture is 0.22, the focal length is 10 mm, the beam diameter is 5 mm, the beam divergence angle is less than 2° and the working wavelength range is from 200–2500 nm.

In order to verify the feasibility of the reflection probe system, a transmission optical probe was designed as well. Fig. 3(c) shows the schematic of the transmission optical probe system.

Under the same condition, the effects of the two reflection systems were tested, and the results are shown in Fig. 3(d). As can be seen, both curves show the same spectrum characteristics except the difference in digital number (DN). And the reason for the unsmooth connection at the wavelength of 1100 nm is that it is spliced by two spectrometers, and 1100 nm is selected as the splicing point. In general, the DN value obtained by the optical fiber collimator is lower than that obtained by the reflection collimator. Although the reflection collimator has a good collimation effect and can detect the distance of the samples, it is difficult to install and debug because of its structure and heavy weight. The optical fiber collimator has been satisfied to use in Fig. 3(d). And that the installation and debugging mode are relatively simple and the price is relatively low. In view of this, the optical fiber collimator was adopted for the following spectrum experiments.

### 3. Results and discussion

Fig. 4 shows the testing results for the weight and the Karl-Fisher method. As can be seen, the moisture content measured by Karl-Fisher is significantly higher than that measured by the weight method. This is because the moisture content in the fresh lubricating oil

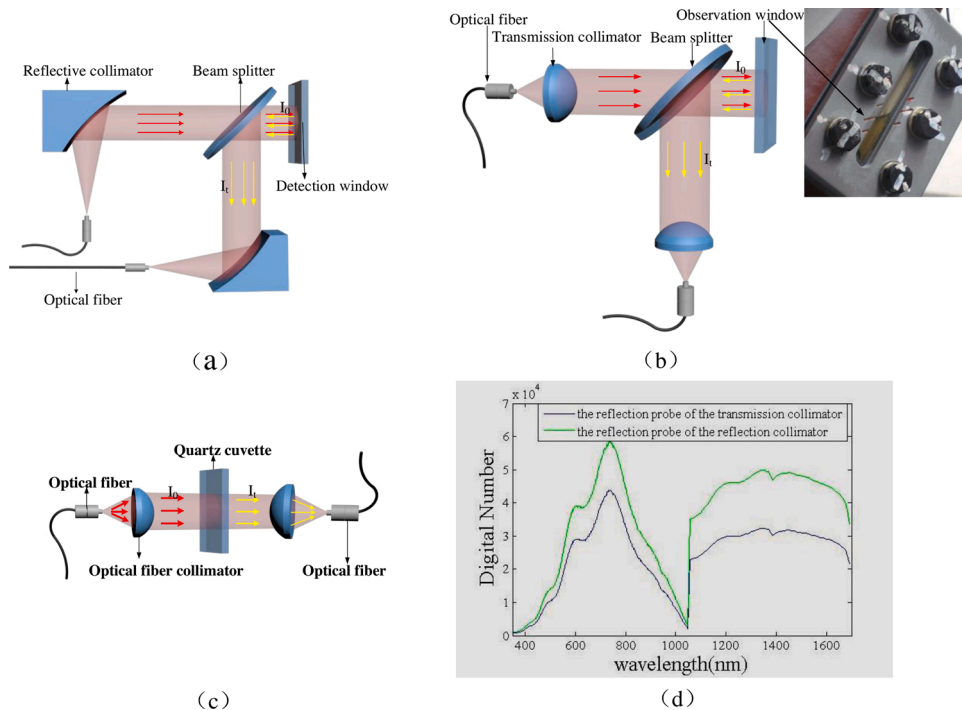


Fig. 3. The reflection and transmission probing system. (a) The reflection probe uses a reflective mirror as collimator, (b) The reflection probe uses an optical fiber collimator as collimator, (c) The transmission probe system, (d) Spectral curves obtained with the reflection probe system.

is about 439.53 ppm. As can be seen, the difference in moisture content obtained by two methods is about the same. However, the trend or the slope of both curves keep the same. Therefore, the measurement result obtained by coulometric Karl Fischer titration was used for the data regression fitting in the subsequent data processing step. In our experiment, 150 samples with different water contents ranging from 100 ppm to 1500 ppm with a 100 ppm step were prepared. In order to reduce the measurement error, each sample was divided into 10 equal parts and as a result there are 150 parts in total. In Fig. 4, 16 samples with different moisture contents were prepared in order to compare different calibration methods, i.e. the weight method and the Karl-Fisher method. Based on the comparison result, Karl-Fisher method was selected as the standard and more accurate method to prepare the samples. In the following regression algorithm, all 150 samples were still used to improve the accuracy of inversion. Out of which, 120 samples were randomly selected as the calibration set and the remaining 30 samples as the prediction set.

Fig. 5 shows the measured absorption spectra of lubricating oils with different water concentration by using both reflection and transmission probing systems. As can be seen, both probing methods can obtain the same spectrum characteristic with consistent absorption peaks. More specifically, there are obvious absorption peaks at wavelength of 405 nm, 970 nm, 1180 nm and 1400 nm. The absorption peaks in the vicinity of wavelength 970 nm, 1180 nm, 1400 nm correspond to vibrational spectrum caused by the O—H bond stretching. However, the absorbance of the reflection system is much higher than that of the transmission system, which is because the light path of the reflection probing system is twice that of the transmission probing system approximately. Therefore, the reflection probing system has a much higher dynamic measurement range. In the following, the measurement results were analysed by employing SPA-PLSR and SPA-BPNN algorithms.

The first step for spectra analysis is the spectrum curve preprocessing, which was done by employing the mahalanobis distance method. The main purpose of the step is to eliminate abnormal samples, which can improve the stability of modeling. Next, the Savitzky-Golay convolution smoothing was conducted on the curve, which intends to emphasize the central role of the center point. This method adopts polynomial least squares to fit the data in the moving window, which can improve the smoothness of the spectrum so that the noise interference can be suppressed. At the same time, the derivative spectrum method was also employed to effectively eliminate the interference from baseline and other backgrounds, which makes it easier to distinguish overlapping peaks so that the spectral resolution can be improved. After preprocessing, the successive projections algorithm (SPA) is adopted to choose characteristic variables [28,29]. This method is a forward selection method which uses simple operations in a vector space to minimize the inter-variable collinearity. The variables with the maximum projection are selected as the new feature variables through orthogonal projection transformation. The extracted characteristic variables represent the useful part of original spectral information and thus the redundant variables can be efficiently eliminated to simplify the model further. Though the correction set model based on SPA has a high accuracy, the accuracy for the prediction set model is not high enough. One possible reason is that the selected variables couldn't provide enough useful information to the model, and as a result a high prediction accuracy couldn't be obtained.

Furthermore, partial least square regression (PLSR) was employed for spectra analysis in this work [30]. PLSR is a perfect method which allows to combine multiple linear regression, canonical correlation analysis and principal component analysis together and thus is widely used in spectral modeling analysis. In the PLSR algorithm, the matrix decomposition and regression are implemented in the same step. The data matrix  $X(n, m)$  is formed by Vis-NIR spectra of the lubricant samples acquired by spectroscopic instruments and the vector  $y(n, 1)$  contains the values for the moisture content, where  $n$  is the number of samples in the calibration dataset and  $m$  is the number of wavelengths of the Vis-NIR spectra.

$$X = TP^T + E \tag{2}$$

$$y = Tq^T + f \tag{3}$$

Where the  $E(n, m)$  and  $f(n,1)$  are the residuals of  $X$  and  $y$ , respectively.  $p$  is the loading matrix of  $X$  and  $q$  is the loading vector of  $y$ .

That is to say, the decomposition of spectral matrix and the concentration matrix is carried out simultaneously. This can be done by introducing the concentration matrix into the spectral matrix so that the principal component of the obtained spectral matrix is directly related to the concentration matrix. In this way, a new principal component of the spectral matrix can be obtained by exchanging the

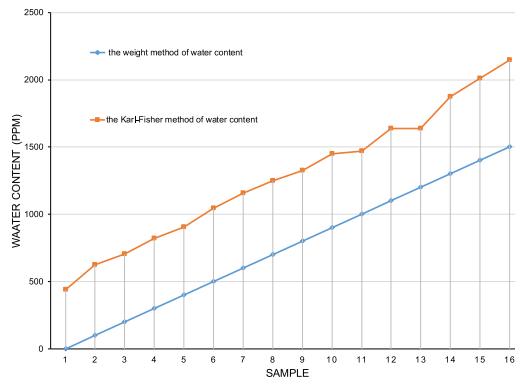
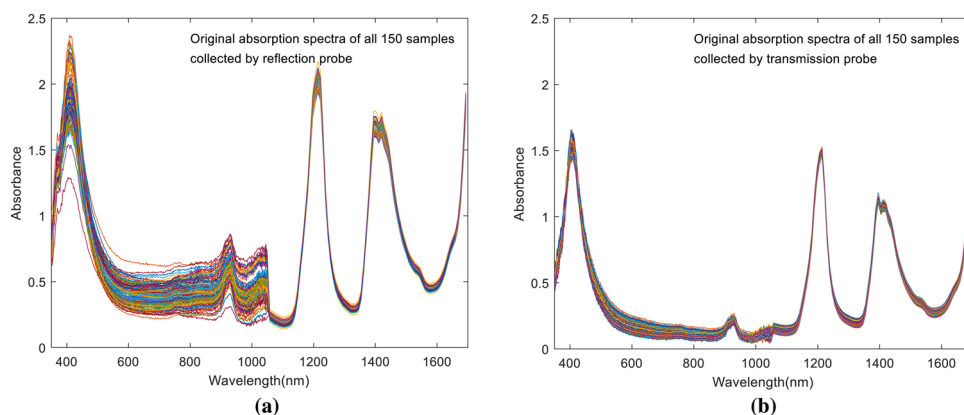
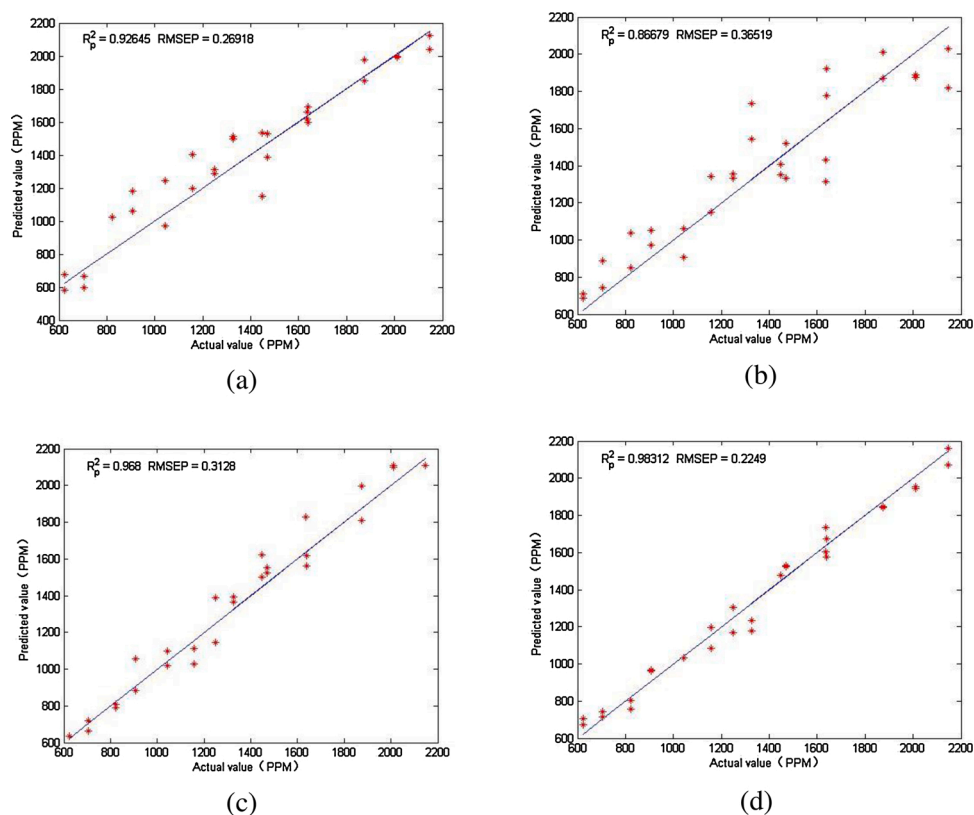


Fig. 4. Moisture content obtained by weight method and Karl-Fisher method.



**Fig. 5.** The absorption spectra of 150 lubricating oils samples with different moisture concentrations measured by reflection (a) and transmission (b) probing systems.

score of the spectral matrix with that of the concentration matrix. PLSR is based on the assumption of a multi-variate correction method for linear regression, and it obeys the Beer-Lambert Law. However, there is a certain non-linear relationship between the absorption spectral parameters and the measurement values of the sample concentration, especially when the dynamic range of the sample concentration is quite large. To solve this problem, neural network algorithm was introduced in this work. The artificial neural network, which imitates the human neural activity to establish the mathematical modeling of neural activity, has the advantages of self-learning, self-organizing and self-adapting so that it has a great fault tolerance and a highly nonlinear expression. Back propagation neural networks (BPNN), which is often used for near infrared spectroscopy, is a multilayer feed forward neural network. Its main characteristics are signal forward transmission and error back propagation [31,32]. In our experiment, a seven-layer BPNN model with a sigmoid function for the hidden layer, a maximum training parameter of 1000 and a linear function for the output layer



**Fig. 6.** Modelling results by PLSR and BPNN methods. (a) PLSR model for transmitted spectra; (b) PLSR model for reflection spectra; (c) BPNN model transmitted spectra; (d) BPNN model for reflection spectra.

are employed.

Normally, evaluation parameters such as prediction standard deviation and determination coefficient will be used in the process of modeling for verification. The standard prediction error (*RMSEP*) is expressed by,

$$RMSEP = \sqrt{\frac{\sum_{i=1}^n (y_{i,actual} - y_{i,predicted})^2}{m - 1}} \quad (4)$$

Where  $y_{i,actual}$  is the measurement value of the  $i_{th}$  sample reference method,  $y_{i,predicted}$  is the predicted value of the  $i_{th}$  sample in the process of verifying set prediction,  $m$  is the number of samples of the verification set. The smaller the standard prediction error, the stronger the prediction ability of the model.

Coefficient of determination ( $R^2$ ) is expressed by,

$$R^2 = 1 - \frac{\sum_{i=1}^n (y_{i,actual} - y_{i,predicted})^2}{\sum_{i=1}^n (y_{i,actual} - \bar{y}_{actual})^2} \quad (5)$$

Where,  $\bar{y}_{actual}$  is the average value of the sample reference methods,  $n$  is the number of samples for calibration or validation sets. The closer the coefficient of determination ( $R^2$ ) gets to 1, the higher the accuracy of the model. The experimental error mainly comes from the spectra offset and the measurement error of the standard samples. These errors will accumulate to the inversion results of the regression algorithm.

Based on above mentioned PLSR and SPA-BPNN methods, measured spectra data shown in Fig. 5 were processed and analysed. Fig. 6 shows a comparison of the inversion results between the transmitted and reflection spectra processed by PLSR and BPNN algorithms respectively. The modeling results based on PLSR method is shown in Fig. 6(a) and 6(b). As can be seen, the prediction coefficient of determination ( $R_p^2$ ) for the transmission and reflection systems is 0.92645 and 0.86679 respectively. It means the model based on the transmission system has a stronger prediction ability than reflection system. This is also confirmed by the standard prediction error which is 0.26918 and 0.36519 for transmission and reflection systems respectively. The smaller prediction error is obtained by transmission system. However, the predictive deterministic coefficients for both systems are larger than 0.85, which means that both systems are approximately subjected to Lambert Beer's law and it also indicates the feasibility of the reflection system.

To further improve the accuracy for the reflection system, SPA-BPNN algorithm was employed for modeling and the results are shown in Fig. 6(c) and 6(d). As can be seen, the prediction coefficient of determination ( $R_p^2$ ) for the transmission and reflection systems is 0.968 and 0.98312 respectively and the standard prediction error for the transmission and reflection systems is 0.3128 and 0.2249 respectively. Both values of the prediction coefficient and values of the standard prediction error for the reflection system are better than those of the transmission system. It means that the model of the reflection system based on neural network has a higher accuracy than that of the transmission system. Moreover, models based on the neural network for both systems are better than PLSR. The possible reason is that the light path in the reflection system is longer than that of the transmission system, which leads to an increase in nonlinear information. Whereas, neural networks can incorporate more nonlinear information into the model than PLSR. As a result, the model of the reflection system based on neural network has a higher accuracy than that of the transmission system.

#### 4. Conclusion

In summary, we demonstrated the feasibility of Vis-NIR spectroscopy method for measurement of the lubricating oil contaminants for gearbox of high-speed rail. For the purpose of real-time monitoring through viewport of gearbox, the reflection probing system was designed and realized. Both the measuring and modeling results show that the reflection probing system works well and agrees well with the transmission system. In particular, it was shown that the model for reflection system based on neural network algorithm works better than transmission system. As a result, the Vis-NIR spectroscopy method was shown to be feasible for lubricating oil contaminants tests, which provides a convenient and fast way for real-time monitoring of the safety of the high-speed rail. However, the current results were obtained in laboratory and obviously more works must be done to make this method more practical for the real working conditions.

#### Declaration of Competing Interest

The authors declare that they have no known competing financial interests or personal relationships that could have appeared to influence the work reported in this paper.

#### Acknowledgements

This work was supported by the National Key Research and Development Program of China [No. 2017YFC1403700]; and the Natural Science Foundation of China [No. 61475156 and No.61361166004].

## References

- [1] R.H. de Paula Pedroza, J.T.N. Nicácio, B.S. dos Santos, K.M.G. de Lima, Determining the kinematic viscosity of lubricant oils for gear motors by using the near infrared spectroscopy (NIRS) and the wavelength selection, *Anal. Lett.* 46 (7) (2013) 1145–1154.
- [2] W.G. Hu, Z.M. Liu, D.K. Liu, X. Hai, Fatigue failure analysis of high speed train gearbox housings, *Eng. Fail. Anal.* 73 (2017) 57–71.
- [3] S. Zzeyani, M. Mikou, J. Naja, A. Elachhab, Spectroscopic analysis of synthetic lubricating oil, *Tribol. Int.* 114 (2017) 27–32.
- [4] S. Soni, M. Agarwal, Lubricants from renewable energy sources – a review, *Green Chem. Lett. Rev.* 7 (4) (2014) 359–382.
- [5] L.M. de Souza, H. Mitsutake, L.C. Gontijo, W. Borges Neto, Quantification of residual automotive lubricant oil as an adulterant in Brazilian S-10 diesel using MIR spectroscopy and PLS, *Fuel* 130 (2014) 257–262.
- [6] R.Q. Aucelio, R. Souza, R.C. M.; de Campos, N. Miekeley, C.L.P. da Silveira, The determination of trace metals in lubricating oils by atomic spectrometry, *Spectrochim Acta B* 62 (9) (2007) 952–961.
- [7] J.W.B. Braga, A.A. dos Santos, I.S. Martins, Determination of viscosity index in lubricant oils by infrared spectroscopy and PLSR, *Fuel* 120 (2014) 171–178.
- [8] M. Blanco, J. Coello, H. Iturriaga, S. Maspocho, R. Gonzalez, Determination of water in lubricating oils by mid- and near-infrared spectroscopy, *Mikrochim. Acta* 128 (3–4) (1998) 235–239.
- [9] R.E. Cantley, The effect of water in lubricating oil on bearing fatigue life, *ASLE Transactions* 20 (3) (1977) 244–248.
- [10] D. Jackson, The spectrographic analysis of Lubricating Oils, *Anal. Chem.* 26 (10) (1954), 1664–1664.
- [11] K.W. Jackson, K.M. Aldous, D.G. Mitchell, Simultaneous determination of trace wear metals in used lubricating oils by atomic-absorption spectrometry using a silicon-target vidicon detector, *Appl. Spectrosc.* 28 (6) (1974) 569–573.
- [12] A.G. Mignani, L. Ciaccheri, N. Díaz-Herrera, A.A. Mencaglia, H. Ottevaere, H. Thienpont, S. Francalanci, A. Paccagnini, F.S. Pavone, Optical fiber spectroscopy for measuring quality indicators of lubricant oils, *Meas. Sci. Technol.* 20 (3) (2009), 034011.
- [13] C.T. Pinheiro, R. Rendall, M.J. Quina, M.S. Reis, L.M. Gando-Ferreira, Assessment and prediction of lubricant oil properties using infrared spectroscopy and advanced predictive analytics, *Energy Fuels* 31 (1) (2016) 179–187.
- [14] X.L. Zhu, L. Du, B.D. Liu, J. Zhe, A microsensor array for quantification of lubricant contaminants using a back propagation artificial neural network, *J. Micromech. Microeng.* 26 (6) (2016), 065005.
- [15] R. Nadkarni, R. Nadkarni, Guide to ASTM test methods for the analysis of petroleum products and lubricants, ASTM International West Conshohocken (2007).
- [16] X. Meng, J. Sedman, F.R. van de Voort, Improving the determination of moisture in edible oils by FTIR spectroscopy using acetonitrile extraction, *Food Chem.* 135 (2) (2012) 722–729.
- [17] E.P. Ng, S. Mintova, Quantitative moisture measurements in lubricating oils by FTIR spectroscopy combined with solvent extraction approach, *Microchem. J.* 98 (2) (2011) 177–185.
- [18] M. Holzki, H. Fouckhardt, T. Klotzbucher, Evanescent-field fiber sensor for the water content in lubricating oils with sensitivity increase by dielectrophoresis, *Sensor Actuat a-Phys* 184 (2012) 93–97.
- [19] S. Raadnui, S. Kleesuwana, Low-cost condition monitoring sensor for used oil analysis, *Wear* 259 (7–12) (2005) 1502–1506.
- [20] C. Burgess, A. Knowles, Standards in Absorption Spectrometry, Vol. 1, CRC Press, 1981.
- [21] B.D. Sacko, S. Sanogo, H. Konare, A. Ba, T. Diakite, Capability of visible-near infrared spectroscopy in estimating soils carbon, potassium and phosphorus, *Opt. Photonics J.* 08 (05) (2018) 123–134.
- [22] Z. Pittaki-Chrysodonta, P. Moldrup, M. Knadel, B.V. Iversen, C. Hermansen, M. Greve, L.W. H.; de Jonge, Predicting the campbell soil water retention function: comparing visible–near-infrared spectroscopy with classical pedotransfer function, *Vadose Zone J.* 17 (1) (2018) 0.
- [23] J. Liu, J. Han, Y. Zhang, H. Wang, H. Kong, L. Shi, Prediction of soil organic carbon with different parent materials development using visible-near infrared spectroscopy, *Spectrochim. Acta A. Mol. Biomol. Spectrosc.* 204 (2018) 33–39.
- [24] R. Khodabakhshian, B. Emadi, M. Khojastehpour, M.R. Golzarian, A. Sazgarnia, Non-destructive evaluation of maturity and quality parameters of pomegranate fruit by visible/near infrared spectroscopy, *Int. J. Food Prop.* 20 (1) (2016) 41–52.
- [25] Z. Basati, B. Jamshidi, M. Rasekh, Y. Abbaspour-Gilandeh, Detection of sunn pest-damaged wheat samples using visible/near-infrared spectroscopy based on pattern recognition, *Spectrochim. Acta A. Mol. Biomol. Spectrosc.* 203 (2018) 308–314.
- [26] F.S.G. Lima, M.A.S. Araújo, L.E.P. Borges, Determination of the carcinogenic potential of lubricant base oil using near infrared spectroscopy and chemometrics, *Tribol. Int.* 36 (9) (2003) 691–696.
- [27] D. Zamora, M. Blanco, M. Bautista, R. Mulero, M. Mir, An analytical method for lubricant quality control by NIR spectroscopy, *Talanta* 89 (2012) 478–483.
- [28] M.C.U. Araujo, T.C.B. Saldanha, R.K.H. Galvao, T. Yoneyama, H.C. Chame, V. Visani, The successive projections algorithm for variable selection in spectroscopic multicomponent analysis, *Chemom. Intell. Lab. Syst.* 57 (2) (2001) 65–73.
- [29] R.K.H. Galvao, M.F. Pimentel, M.C.U. Araujo, T. Yoneyama, V. Visani, Aspects of the successive projections algorithm for variable selection in multivariate calibration applied to plasma emission spectrometry, *Anal. Chim. Acta* 443 (1) (2001) 107–115.
- [30] P. Geladi, B.R. Kowalski, Partial least-squares regression - a tutorial, *Anal. Chim. Acta* 185 (1986) 1–17.
- [31] S. Ferrari, R.F. Stengel, Smooth function approximation using neural networks, *IEEE T Neural Networ* 16 (1) (2005) 24–38.
- [32] Y.Q. Ni, M. Li, Wind pressure data reconstruction using neural network techniques: a comparison between BPNN and GRNN, *Measurement* 88 (2016) 468–476.